

Three-dimensional Modeling of the Matter Flow Structure in Semidetached Binary Systems

D.V.Bisikalo¹

Institute of Astronomy of the Russian Acad. of Sci., Moscow, Russia

A.A.Boyarchuk

Institute of Astronomy of the Russian Acad. of Sci., Moscow, Russia

O.A.Kuznetsov²

Keldysh Institute of Applied Mathematics, Moscow, Russia

V.M.Chechetkin

Keldysh Institute of Applied Mathematics, Moscow, Russia

ABSTRACT

Results of numerical simulations of matter flows in a semidetached binary system similar to the low-mass X-ray binary X1822–371 are presented. Three-dimensional modeling of the mass transfer gas dynamics makes it possible to investigate gas streams in the system and to study the influence of a common envelope. The presence of the common envelope leads to the absence of shock interaction between the stream of matter flowing from the inner Lagrange point and the gas in the accretion disk. The stream is deflected by the gas in the common envelope and approaches the disk tangentially, so that it does not cause any shock perturbation (“hot spot”) on the disk. At the same time, the interaction of the stream with the common envelope leads to the formation of an extended shock wave along the edge of the stream. The observational manifestation of this shock is estimated to be equivalent to that of a hot spot in the disk. The calculated accretion disk parameters are presented.

¹E-mail address: bisikalo@inasan.rssi.ru

²E-mail address: kuznecov@spp.keldysh.ru

1. Introduction

Semidetached binary systems are interacting binaries, in which one of the stars fills its critical surface, resulting in mass exchange between the components of the system. In general, the critical surface has a complicated shape [1], and special mathematical models are required to describe matter flows in the system (a review of such models is given in [2]). However, the large amount of observational data confirming the small eccentricity of the orbits and the high degree of synchronization in these binary systems makes it possible to simplify the models used. In the standard formulation, the components of semidetached binary systems are assumed to have circular orbits and to rotate in synchrony with the orbital motion. In this case, the critical surface is identified with the inner surface (Roche surface) in the restricted three-body problem, and it is assumed that the mass exchange between the system components occurs through the vicinity of the inner Lagrange point L_1 , where the pressure gradient is not balanced by the force of gravity.

The gas dynamics of mass transfer through the inner Lagrange point L_1 have been studied by many authors. A thorough analysis of the flow of matter in the vicinity of L_1 was performed by Lubow and Shu [3], who estimated the basic characteristics of the flow in a semi-analytical approximation using a perturbation method. The small parameter ϵ used in this analysis was the ratio of the sound speed c_0 at the star's surface to the characteristic orbital velocity ΩA (Ω is the angular velocity of rotation of the system components and A is the distance between the component centers). In another approach based on Bernoulli integral analysis, the parameters of the stream of matter were refined, and a relationship obtained between the mass transfer rate and the degree of overfilling of the Roche lobe by the donor star [4,5].

To adequately describe the mass exchange process, it is necessary, in addition to determining the stream parameters, to consider the further behavior of the stream lines after the motion of matter from L_1 . It is the mass transfer process that forms the overall pattern of the flow and, consequently, defines its basic observational manifestations; therefore, much attention has been given to the study of this problem. Warner and Peters [6], Lubow and Shu [3], and Flannery [7] pioneered the investigation of particles ejected from L_1 and moving in the gravitation field of the binary

system. The results obtained in these and a number of subsequent studies have gained wide recognition, but their application to the analyses of specific systems led to the discovery of substantial discrepancies with the observational data. These discrepancies are associated with the use of a simplified ballistic approach in the gas motion analysis, which did not take into account gas dynamics effects. To consider the influence on gas motions of a circumstellar envelope during and after its formation, and, consequently, to accurately describe matter flows, it is necessary to solve a complete system of gas dynamics equations; this is possible only using quite sophisticated mathematical models.

The use of numerical methods to study the gas dynamics of mass transfer in semidetached binary system was for a long time limited by the development of computer techniques, so that two-dimensional (2D) models were used for the flow analysis. In spite of the simplification of the 2D approach, it enabled a correct treatment of some particular features of the matter flow, and made it possible to obtain a number of interesting results (see, e.g., [8–12]). In recent years, numerical investigations of mass transfer gas dynamics using more realistic three-dimensional (3D) models have become possible [13–20]. Such studies have considered, in particular, accretion disk formation in semidetached binary systems [13, 15], and also the region of interaction between the stream flowing from L_1 and the disk [14, 20]. Unfortunately, these studies were conducted in a limited formulation, without considering the process of establishing the flow on long time scales; this prevented investigation of the real morphology of the systems and, correspondingly, evaluation of the impact of a common envelope on the flow pattern. Some progress in the investigation of the overall flow pattern was achieved in the studies of Molteni, Belvedere, and Lanzafame [16–19], who conducted 3D numerical simulations over rather long time intervals. A number of interesting results were obtained in these papers, however, the use of the Smoothed Particle Hydrodynamics (SPH) method to solve the system of gas dynamics equations made it impossible to study the influence of a common envelope on the flow pattern. The restrictions imposed by the SPH method do not allow investigation of flows with large density gradients, and, therefore, the action of the rarefied envelope gas on the mass transfer gas dynamics was not taken into account entirely correctly.

Here, we present the results of 3D numerical simulations of the flow patterns in semidetached binary systems. The Total Variation Diminishing (TVD) method we use to solve the system of gas dynamics equations does not have the disadvantages of the SPH method. This made it possible to investigate gas flow morphology in the system and the effect of the common envelope of the system, despite the presence of substantial density gradients. We studied the gas dynamics of matter flows in semidetached binary systems over long time intervals, which enabled us to consider the basic features of the flow pattern in a steady-state (stationary) regime.

2. The Model

2.1. Physical Model

Semidetached binary systems exhibiting extremely interesting observational manifestations of their interaction include cataclysmic binaries, low mass X-ray binaries (LMXB), and supersoft X-ray sources. The available observations of LMXB X-ray light curves provide striking evidence for the presence of complicated flow patterns, and suggest some characteristic features of the gas flow structure. In particular, in a number of X-ray "dipping" sources, of which the most widely known is the X1822–371 system, a substantial decrease of the emission is observed at phase 0.8 of the orbital period, associated with a thickening in the disk in the place where it is perturbed by the stream of gas flowing from L_1 [20–22].

In our studies of matter flow patterns, we considered semidetached binary systems with parameters typical for low mass X-ray binaries, where a main sequence dwarf fills its Roche lobe and transfers mass to a neutron star. For more specific calculations, we chose a system with parameters close to those of X1822–371 [20]. We assumed that the primary star filling its Roche lobe has a mass M_1 equal to $0.28M_\odot$ and a surface gas temperature $T = 10^4 K$; the mass of the companion (a compact object with radius $0.05R_\odot$) has $M_2 = 1.4M_\odot$; the orbital period of the system is $P_{orb} = 1^d78$; and the distance between the centers of the two stars is $A = 7.35R_\odot$.

To adequately describe the matter flow structure in the binary system we have chosen, we must take into account the effect of radiation processes upon the gas dynamics. Including non-adiabatic processes in the numerical model substantially increases the calculation time. For this reason, based on the available

computational resources and the need to let the calculations run over long time intervals (to obtain a steady-state regime for the flow), we restricted our consideration to an ideal gas model with adiabatic index γ and equation of state $P = (\gamma - 1)\rho\varepsilon$ (where P is pressure, ρ is density, and ε is specific internal energy). The ideal gas assumption in the model formally neglects radiative losses; however, in the calculations presented, the adiabatic index was assumed to be close to unity (namely, $\gamma = 1.01$), which approaches the isothermic case [23]. This, in turn, allows us to treat the $\gamma \sim 1$ model used as a system with energy losses. A similar technique for taking into account radiative losses is well known and has been applied in a number of studies (see, for example, [16, 24]). This procedure clearly prevents accurate allowance for radiative cooling of gas in the system, but, nonetheless, brings the model used closer to a realistic case.

2.2. Mathematical Model

We used a 3D system of gas dynamics equations, closed by the ideal gas equation of state with adiabatic index $\gamma = 1.01$, to describe the gas flow. We used an integral form of this system, since these equations allow, together with continuous solutions, non-isoentropic solutions satisfying the Rankin–Hugoniot conditions at discontinuities (shock waves and contact discontinuities). The system has the form

$$\begin{aligned} \frac{\partial}{\partial t} \int_V \rho \, dV + \int_\Sigma \rho(\mathbf{v} \cdot \mathbf{n}) \, d\Sigma &= 0 \\ \frac{\partial}{\partial t} \int_V \rho \mathbf{v} \, dV + \int_\Sigma \rho \mathbf{v}(\mathbf{v} \cdot \mathbf{n}) \, d\Sigma + \int_\Sigma P \mathbf{n} \, d\Sigma &= \int_V \rho \mathbf{F} \, dV \\ \frac{\partial}{\partial t} \int_V \rho E \, dV + \int_\Sigma \rho h(\mathbf{v} \cdot \mathbf{n}) \, d\Sigma &= \int_V \rho(\mathbf{F} \cdot \mathbf{v}) \, dV \quad . \end{aligned}$$

The specific external force \mathbf{F} includes the Coriolis force, and also the attractive force of the two gravitational centers and the centrifugal force (both described by the Roche potential). It has the form

$$\mathbf{F} = -\text{grad } \Phi + 2[\mathbf{v} \times \boldsymbol{\Omega}] \quad ,$$

where the Roche potential can be written

$$\Phi(\mathbf{r}) = -\frac{GM_1}{|\mathbf{r} - \mathbf{r}_1|} - \frac{GM_2}{|\mathbf{r} - \mathbf{r}_2|} - \frac{1}{2}\Omega^2(\mathbf{r} - \mathbf{r}_c)^2 \quad .$$

Here, \mathbf{v} is the velocity, $\mathbf{\Omega} = (0, 0, \Omega)$, $\Omega = 2\pi/P_{orb}$, \mathbf{r}_1 and \mathbf{r}_2 are the centers of the system components, and \mathbf{r}_c is the center of mass of the system.

We adopted the following boundary conditions.

(1) The outflowing star fills its Roche lobe. Over the entire surface of this component, the gas velocity is normal to the surface. The gas speed is assumed to equal the local sound speed $v = c_0 = 9\text{km/s}$.

(2) The conditions of free matter outflow are set both on the accretor and at the outer boundary.

(3) The density ρ in the outflowing component's Roche lobe was taken to be ρ_0 . Note that the boundary value of the density in the outflowing component does not affect the solution, since the system of equations scales with ρ and P . We used an arbitrary value for ρ_0 in the calculations. However, when a specific system with a known mass loss rate is considered, the real density values can be found simply by adjusting the calculated density values according to the scale implied by the ratio of the real and model densities at the surface of the outflowing component.

We took the gas in the calculation region to initially have low density and be at rest. This gas is later displaced by the gas flowing outward from the primary component.

2.3. Numerical Model

A fundamental problem in the numerical realization of gas dynamics models is the choice of a method for solution of the corresponding system of equations. Currently, finite difference methods recommend themselves most highly. Of the wide variety of finite difference schemes, the most accurate are so-called Godunov methods [25]. These are based on approximating the initial gas dynamics equations in divergence form (corresponding to the conservation laws), which makes it possible to obtain correct values at discontinuities in the case of discontinuous solutions. The important features of finite difference methods, which, in many respects, determine the resulting adequacy of the solutions, are the approximation viscosity and the monotonicity of the scheme. Increasing the approximation order decreases the numerical viscosity. It is possible to decrease the numerical viscosity in a scheme with a given order using characteristic properties of the initial system of gas dynamics equations, which is hyperbolic. This approach leads to so-called Total Variation Diminishing (TVD) schemes, which have the property of mono-

tonicity (corresponding to the absence of nonphysical oscillations of the solutions near discontinuities) [26]. Increasing the approximation order and introducing special flow restrictions that make it possible to preserve the monotonicity lead to high-order TVD methods with minimal approximation viscosity [27]. In spite of their relative complexity, such schemes are currently the most promising for the numerical realization of gas dynamics models.

We used a high-order TVD scheme to numerically solve the system of equations. Special studies showed that this method makes it possible to adequately reflect flow structures that include shock waves and tangential discontinuities, without leading to artificial oscillations or smearing of features in the flow pattern. In addition, the method allows us to study flows with large density gradients, which is especially important when treating the influence of common envelope gas on the flow structure.

We solved the gas dynamics equations in a Cartesian coordinate system specified as follows:

- origin at the center of the outflowing star;
- X axis directed along the line connecting the star centers, from the outflowing component to the accretor;
- Z axis directed along the rotation axis;
- Y axis defined so that the resulting system is right-handed.

The calculation region is the parallelepiped $(-A..2A) \times (A..A) \times (0..A)$; by virtue of the symmetry of the problem, we carried out the calculations only for the upper half-space. We used a non-uniform (denser in the accretor zone) difference grid with $78 \times 69 \times 35$ nodes for the numerical calculations.

The system of equations was solved using a method for transition to a steady state, from arbitrarily chosen initial conditions to the entry of the solution to a stationary regime. Note that the characteristic gas dynamics timescale for the establishment of the flow for the system under consideration (the ratio of the system's characteristic size A to the propagation velocity of perturbations c_0) is of the order of three orbital periods. Thus, to ensure that the resulting solution was stationary, we carried out the calculations over a substantially longer time interval — more than ten orbital periods. We checked the degree of stationarity of the solution using both local and integrated characteristics of the flow.

3. Calculation Results

We will consider some characteristic features of the flow structure in semidetached binary systems obtained using the 3D gas dynamics model described in Section 2. The overall flow pattern, which illustrates the morphology of gas flows in the system, is shown in Fig. 1, which presents three-dimensional images of density contours at the levels of 0.01 (Fig. 1a) and 0.05 (Fig. 1b) of the gas density at the point L_1 . To better show details of the calculated flow structure, Fig. 2 shows cross sections of the density contours in Fig. 1a made by the XZ and YZ planes passing through the accretor. The flow pattern in Fig. 1 and Fig. 2 is time steady, and corresponds to the steady flow regime achieved after a time interval exceeding ten orbital periods from the starting time of the calculations. These results reveal the following features of the calculated flow structure.

1) The matter of the stream can be conditionally divided into three parts: the first forms a quasi-elliptical accretion disk; the second bends around the accretor and, remaining inside the system, acts upon the overall flow pattern; and the third leaves the system through the vicinity of Lagrange point L_2 .

2) The interaction between the stream and the disk is not a shock interaction.

3) The dimensions of the stream of matter flowing from the vicinity of L_1 change as the stream propagates toward the accretor: its height decreases and its width in the orbital plane increases.

4) The height of the accretion disk that forms in the system is much less than the height of the stream; this is confirmed by the data presented in Fig. 3, which shows density contours up to the value $\rho \sim 0.01\rho_0$ and velocity vector in the YZ plane, which forms a transverse cut through the disk when it passes through the accretor.

We can analyze the structure of gas flows in more detail and estimate the disk's linear size by considering the flow pattern in the equatorial plane. Figure 4 presents the density field and velocity vector field in this plane inside an area with dimensions from 2 to $10R_\odot$ along the X axis and from -3 to $3R_\odot$ along the Y axis. Four stream lines, marked with the letters A, B, C, D and indicating the directions of flows in the system, are also shown. Analysis of the results presented in Fig. 4 confirms the above conclusion that some of the stream material leaves the system through the vicinity of the Lagrange point L_2 without getting

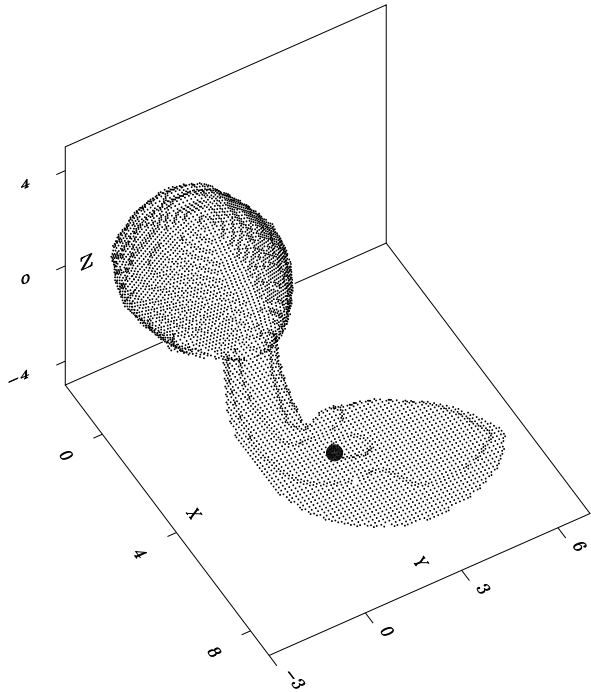


Fig. 1a.— 3D view of density isosurface at the level $\rho = 0.01\rho_0$. X, Y, Z are given in units of R_\odot . The location of the accretor is marked by the dark circle.

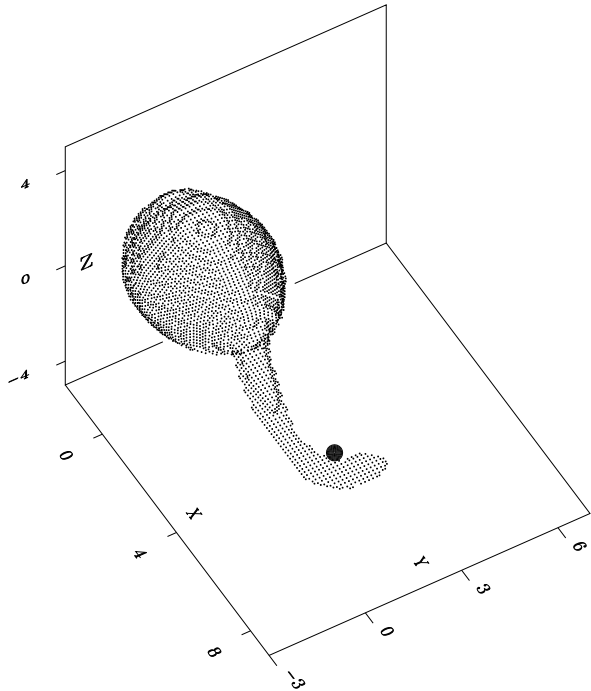


Fig. 1b.— 3D view of density isosurface at the level $\rho = 0.05\rho_0$.

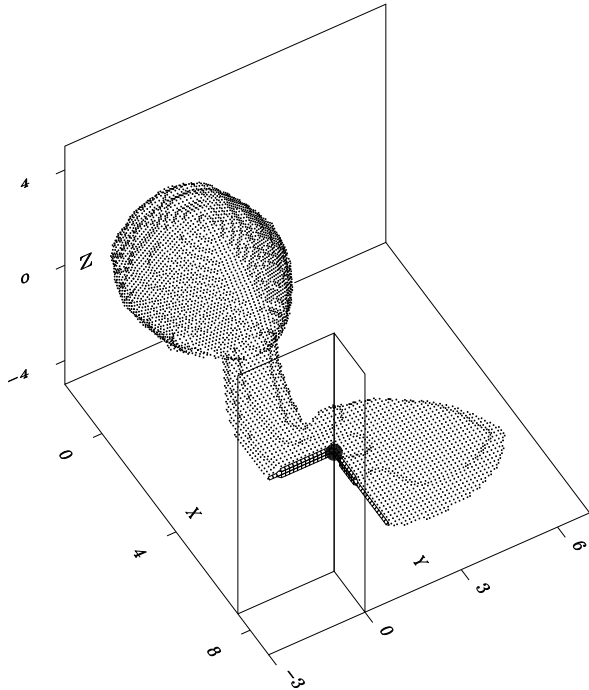


Fig. 2.— The same density isosurface as on Fig. 1a, sliced by the XZ and YZ half-planes passing through the accretor.

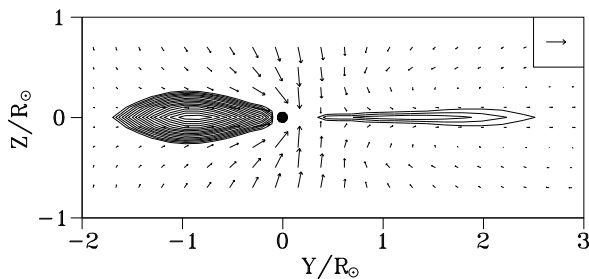


Fig. 3.— Density isolines and velocity vectors in the plane YZ passing through the accretor. The filled circle with the center in the point $y = 0, z = 0$ marks the location of the accretor. Vector in the upper right corner corresponds to the value of velocity of 1000 km/sec.

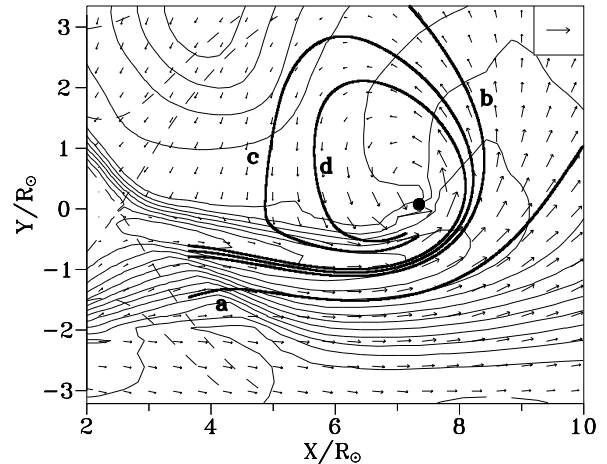


Fig. 4.— Density isolines and velocity vectors in the equatorial plane of the system. The Roche equipotentials are shown with dashed lines. Four stream lines marked with the letters A, B, C, and D are also shown. The accretor position is marked with the dark circle. The vector in the upper right corner corresponds to a velocity of 800 km/s.

close to the accretor (stream line A). Some material falls directly onto the disk (stream line D) and further, losing its angular momentum under the action of viscosity, takes part in the accretion process. The quantitative estimates obtained indicate that about 75% of gas injected into the system is accreted.

Of the most interest for the purposes of this paper is the material that acts upon the flow pattern while remaining inside the system (stream lines B and C in Fig. 4). We will call this material the "common envelope" of the system. Note that a significant part of the common envelope gas (see stream line B) bends around the donor star and interacts with the matter outflowing from its surface. The influence of this part of the common envelope on the flow structure leads to substantial changes in the mass exchange regime in the system. We will provide a detailed consideration of this effect in a future paper. Another part of the common envelope (see stream line C) passes completely around the accretor and undergoes a shock interaction with the edge of the stream facing into the orbital motion. This type of interaction results in substantial changes in the overall flow pattern, in particular, in the absence of a "hot spot" in the disk and the formation of an extended shock wave along the edge of the stream. We present a detailed description

of the impact of this part of the common envelope on the gas flow morphology in the system below.

To determine the linear dimensions of the disk, we must find the limiting ("last") stream line along which matter flows directly onto the disk. The preceding stream line (between lines C and D), which directs matter around the accretor and then back to interact with the stream, still passes outside the disk. The matter along this line belongs to the common envelope and not to the disk, although later (after interaction with the stream), it can also be accreted. The limiting stream line in Fig. 4 is D, and we can easily estimate the dimensions of the calculated quasi-elliptical disk by examining this line: $3.2 \times 2.5R_{\odot}$. It follows from Fig. 3 that the disk thickness increases with distance from the accretor, varying from ~ 0.1 to $\sim 0.2R_{\odot}$. Note that to determine the disk thickness more accurately, we must increase the number of grid nodes, since the minimum calculated thickness of the disk was limited by the size of a difference cell.

The variations of the parameters for the gas flowing along the stream lines presented in Fig. 4 show that the flow is smooth along all lines belonging to the disk, up to the limiting line D. The absence of discontinuities indicates a shockless interaction between the stream and disk material, which, in turn, implies the absence of a hot spot in the disk. The results presented in Figs. 1, 2 and 4 provide an explanation for this shockless morphology for the stream-disk system. Examination of the flow pattern makes it clear that the stream deflected by the action of the common envelope gas (stream line C in Fig. 4) approaches the disk along a tangent, and, therefore, does not cause any shock perturbation at the disk surface. At the same time, the interaction of the stream with the common envelope leads to the formation of an extended shock wave along the edge of the stream facing into the orbital motion. We can estimate the shock parameters, as well as the total amount of energy released in the shock, using the calculation results. One of the characteristic features of the shock is its variable intensity. This is illustrated in Fig. 5, which presents the distribution of the specific rate of energy release along the shock in the equatorial plane δE , normalized to unity. The vertical dashed lines in Fig. 5 show the edges of the stream: the left line shows the point where the stream originates (the point L_1), and the right line the place where the stream ends, i.e., the place where the stream comes into contact with the disk. We can easily seen in Fig. 5 that the bulk of the

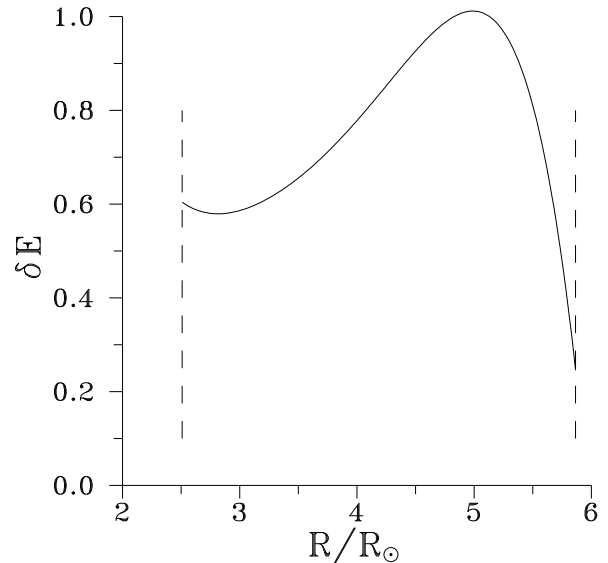


Fig. 5.— Distribution of the specific rate of energy release δE along the shock wave in the equatorial plane, normalized to unity. The dashed lines mark the shock boundaries.

energy in the system is released in the compact shock region, adjacent to the accretion disk. This is extremely important for interpretations of observational data, because the compactness of the energy release region can explain the phase relations of features in binary light curves in essentially the same way as has been done previously assuming the presence of a hot spot, in the framework of a fundamentally different model for the matter flow in the system.

To verify that the shock forming along the edge of the stream is an adequate substitution for the hypothetical hot spot in the disk, let us consider the total energy release in both of these formations. In accordance with standard models, we assume the hot spot to be generated at a distance R_{out} from the accretor. In this case, the energy release resulting from the stream and disk interaction is (see, e.g., [28]):

$$\Delta E_{spot} = \frac{1}{4} \frac{GM_2 \dot{M}}{R_{out}} \quad ,$$

where \dot{M} is the mass loss rate of the donor star. For the adopted values of the density ρ_0 and temperature (sound speed c_0) at the star's surface, the value of \dot{M} in standard models is determined by the relation

$$\dot{M} = \rho_0 c_0 S \quad ,$$

where S is the cross-sectional area of the stream in the vicinity of L_1 [3]. Using these formulas and determining R_{out} from the calculation results given above, assuming the spot is generated at the point where the stream contacts the disk, we estimated ΔE_{spot} for the gas density and temperature at the surface of the donor star adopted in our model. Comparison of the energy release rate in the shock ΔE_{shock} with our ΔE_{spot} estimate shows that ΔE_{shock} is twice ΔE_{spot} . These approximately equal energy release rates and the quite limited size of the region where the bulk of the energy in the shock is released ($\sim 60\%$ of the energy is released in the one-third of the shock that is adjacent to the disk — see Fig. 5), suggests that the observational manifestations of this shock will be roughly equivalent to those of a hot spot in the disk.

Finally, we note that, in spite of the expected similarity of the observational effects of the hypothetical hot spot and our calculated shock wave, the calculated matter flow morphology in semidetached binary systems is fundamentally different from the standard picture, and this, in turn, calls for a reexamination of a number of commonly accepted concepts. For instance, the presence of a common envelope leads to significant changes in the mass transfer rate in the system. In the case considered, the common envelope causes matter to flow from a much (order of magnitude) larger part of the surface of the donor star than is supposed in standard models (this point will be considered more thoroughly in a future paper). This means that for approximately equal energy release rates in the different ("shock wave" and "hot spot") models, the mass exchange rates will be substantially different. Correct concepts about the flow morphology are especially important when interpreting observations, since comparisons between model calculations and observational data can provide information about the system.

4. Conclusion

We have presented the results of 3D numerical simulations of the matter flow pattern in a semidetached binary system similar to the low mass X-ray binary X1822–371. Our results provide evidence for the substantial influence of the rarefied common envelope gas on the structure of gas streams in the system. The common envelope gas interacts with the stream outflowing from the vicinity of L_1 and deflects it, leading to a shockless (tangential) interaction between the

stream and the outer edge of the accretion disk, and, consequently, to the absence of a hot spot in the disk. At the same time, the interaction of the common envelope gas with the stream results in the formation of an extended shock wave of varying intensity along the edge of the stream. A preliminary analysis suggests that the observational manifestations of this shock and the standard hypothetical hot spot are similar, and, therefore, this shock can be considered equivalent to a hot spot in the interpretation of observations.

Note that these results were obtained for a steady flow regime. In a non-stationary regime, when the flow morphology is determined by external factors and is not self-consistent, regions of shock interaction between the disk and the gas stream are also possible. For example, if the disk is already formed before the donor star fills its Roche lobe, a hot spot can be created where the matter stream makes contact with the outer edge of the disk after the mass exchange through the vicinity of L_1 begins. Since a self-consistent solution without a hot spot is expected after a steady-state flow regime is achieved, it is important to determine the life time for the hot spot. It is natural to adopt for its characteristic life time the time required for the amount of matter injected into the system by the stream to become comparable to the accretion disk mass, since after complete mass exchange, the solution will become self-consistent. With mass exchange and accretion disk parameters typical for the system under consideration [20], we expect that the stationary flow regime will already be established after a time of the order of 100 rotation periods. This suggests that the probability of observing a hot spot is extremely low, and all the observational manifestations that have been associated with hypothetical hot spots are, in fact, consequences of energy release in the shock on the stream edge.

In summary, we conclude that correctly taking into account the common envelope in numerical simulations of the gas dynamics of mass transfer in semidetached binary systems has revealed new features of the gas flow structures, which significantly change our concepts of the morphology of flows in these systems.

This work was supported by the Russian Foundation for Basic Research (project code 96-02-16140).

REFERENCES

- [1] Kruszewski, A., 1963, Acta Astron., 1963, 13, 106

- [2] Lubow, S.H., 1993, in Sahade J., McCluskey J.Jr., Kondo Y., (eds) *The Realm of Interacting Binary Stars*. Kluwer Acad. Press, Dordrecht, p. 25
- [3] Lubow, S.H., Shu, F.H., 1975, ApJ, 198, 383
- [4] Paczyński, B., Sienkiewicz, R., 1972, Acta Astron., 22, 73
- [5] Savonije, G.L., 1978, A&A, 62, 317
- [6] Warner, B., Peters, W.L., 1972, MNRAS, 160, 15
- [7] Flannery, B., 1975, MNRAS, 170, 325
- [8] Sawada, K., Matsuda, T., Hachisu, I., 1986, MNRAS, 219, 75
- [9] Sawada, K., Matsuda, T., Inoue, M., Hachisu, I., 1987, MNRAS, 224, 307
- [10] Taam, R.E., Fu, A., Fryxell, B.A., 1991, ApJ, 371, 696
- [11] Blondin, J.M., Richards, M.T., Malinowski, M.L., 1995, ApJ, 445, 939
- [12] Murray, J.R., 1996, MNRAS, 279, 402
- [13] Nagasawa, M., Matsuda, T., Kuwahara, K., 1991, Num. Astrophys. in Japan, 2, 27
- [14] Hirose, M., Osaki, Y., Minishige, S., 1991, PASJ, 43, 809
- [15] Sawada, K., Matsuda, T., 1992, MNRAS, 255, 17
- [16] Molteni, D., Belvedere, G., Lanzafame, G., 1991, MNRAS, 249, 748
- [17] Lanzafame, G., Belvedere, G., Molteni, D., 1992, MNRAS, 258, 152
- [18] Belvedere, G., Lanzafame, G., Molteni, D., 1993, A&A, 280, 525
- [19] Lanzafame, G., Belvedere, G., Molteni, D., 1994, MNRAS, 267, 312
- [20] Armitage, P.J., Livio, M., 1996, ApJ, 470, 1024
- [21] White, N.E., Holt, S.S., 1982, ApJ, 257, 318
- [22] Mason, K.O., 1989, in Proc. 23rd ESLAB Symp. on Two-Topics in X-ray Astronomy, ESA SP-296, p. 113
- [23] Landau, L.D., Lifshitz, E.M., 1959, *Fluid Mechanics*. Pergamon, Elmsford
- [24] Bisikalo, D.V., Boyarchuk, A.A., Kuznetsov, O.A., Popov, Yu.P., Chechetkin, V.M., 1995, Astron. Reports., 39, 325
- [25] Godunov, S.K., 1959, Math. Sbornik, 47, 271
- [26] Roe, P.L., 1986, Ann. Rev. Fluid Mech., 18, 337
- [27] Chakravarthy, S., Osher, S., 1985, AIAA Pap., N 85-0363
- [28] Pringle, J.E., Wade, R.A. (eds) 1985, *Interacting Binary Stars*. Cambridge Univ. Press, Cambridge